

NONLINEAR AEROSOL LIDAR FOR REMOTE DETECTION AND IDENTIFICATION OF BIOAEROSOLS IN CLOUDS

Guillaume Méjean, François Courvoisier, Jérôme Kasparian, Véronique Boutou, Estelle Salmon, Jin Yu, Jean -Pierre Wolf

Teramobile, LASIM, UMR CNRS 5579, Université Claude Bernard Lyon 1, 43 bd du 11 Novembre 1918, F-69622 Villeurbanne Cedex, France, wolf@lasim.univ-lyon1.fr

ABSTRACT

We demonstrate the first non-linear Lidar for range-resolved detection and identification of biological aerosols in the air. Two-photon-excited fluorescence (2PEF) is induced in riboflavin containing particles at a remote location by ultrashort Terawatt laser pulses. 2PEF-Lidar should be more efficient than 1PEF-Lidar for amino acids detection beyond a typical distance of 2 km, because it takes advantage of the higher atmospheric transmission at the excitation wavelengths. 2PEF-Lidar moreover allows size measurement by pump-probe schemes, and pulse shaping may improve the detection selectivity. Since laser-induced filaments are transmitted through aerosols, bioaerosols may be detected even inside dense clouds

1. NONLINEAR AEROSOL LIDAR

The early detection and identification of potentially harmful bioagents in the air has become a major issue for both defence and public security reasons. This requires fast detection of the outbreak location, 3D-mapping of the plume as it propagates, and unambiguous identification of the agents among the broad variety of atmospheric background aerosols. In this letter, we study the application of fluorescence-based Lidar (Light Detection and Ranging) towards these goals. We demonstrate experimentally the first remote detection and identification of bioagent simulants (riboflavin-doped microparticles) in the air by non-linear Lidar.

We used the 5 TW pulses (80 fs, 400 mJ at 800 nm) of the *Teramobile* [1,2] to induce *in-situ* two-photon-excited fluorescence (2PEF) [3] in riboflavin-doped aerosol particles. The bioagent simulants were produced with an aerosol generator located at 45 m from the *Teramobile*. Their size distribution and concentrations were monitored using an optical sizer (Grimm model G 1-108). They consisted of water droplets of 1 μm size in average (typical for bacteria [4]) and containing 0.02 g/l riboflavin. The backward emitted fluorescence and scattered signals are collected by a 20 cm telescope, which focuses the light on a spectrally resolved detector. The returns are recorded as

a function of the photons flight time, providing distance resolution.

Two major reasons motivate the use of ultrashort multi-photon excitation: (1) the better atmospheric transmission at longer wavelengths (decrease of Rayleigh scattering and prevention of molecular absorption such as ozone) and (2) the possibility of simultaneous size measurement by pump-probe schemes [5,6], and coherent excitation with shaped pulses [7,8] to improve the detection selectivity.

The results for 10^{11} W/cm² incident intensity on the target are shown in Fig. 1. The detected 2PEF spectrum clearly identifies the presence of riboflavin containing particles, and the Lidar range resolution allows the precise spatial localization of the biological aerosol plume. The spatial resolution is 45 cm, limited by the fluorescence lifetime of 3 ns for this transition [9]. Notice that the contrast against fluorescence of the background aerosols present in the air at the time of the measurement is excellent. The comparison with pure water microdroplets clearly demonstrates the capability of identifying biological particles from background non-biological ones of the same size. These experiments show that the one photon per pulse detection limit corresponds to a concentration as low as 10 particles per cubic centimeter, for a 10 m spatial resolution.

Using shorter wavelength excitation (around 530 nm) would provide significant advantages as compared to the 800 nm wavelength: (1) the already high sensitivity would be further enhanced by using 2PEF from the amino-acid tryptophan [4,10]. (Trp), the concentration of which is typically 10^4 times higher than riboflavin in bacteria (10^8 Trp molecules in a 1 μm particle [9]), and (2) two-photons at 530 nm would not only excite tryptophan, but also NADH and riboflavin, whose fluorescence features around 320-370 nm, 420-500 nm, and 520-620 nm, respectively, would provide multiple cross-checking biological signatures of the particle [10].

We performed numerical simulations to estimate the performance of a non-linear 2PEF Lidar, compared to a linear 1PEF-Lidar (emission wavelength 266 nm), in the case of tryptophan fluorescence detection. Although ultrashort Terawatt lasers that emit around 530 nm are not commercially available yet, recent developments in

Ytterbium based lasers are very encouraging, reaching up to the Petawatt level (at the fundamental wavelength, to be frequency doubled) in the laboratory. In these simulations, we assumed that the laser intensity decreases only by linear extinction processes (Rayleigh-Mie scattering and absorption from atmospheric molecules) as it propagates in air to the aerosol plume. Rayleigh scattering widely favors longer wavelengths, because of its λ^{-4} dependence. Around 266 nm, the major absorbing molecule in the atmosphere is ozone.

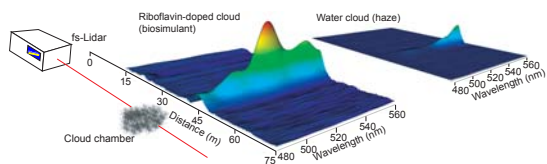


Figure 1: Remote detection and identification of bioaerosols.

We considered particles of 1 μm average diameter containing 10^8 Trp molecules/particle, with the 1-PEF and 2-PEF cross-sections from the literature [9,11,12]. The 1PEF Lidar simulations used the specifications of best commercially available Nd:Yag lasers (fourth harmonic), with 100 mJ at 266 nm and 10 ns pulse duration, while for the 2PEF simulations we used the *Teramobile* laser specifications (400 mJ, 80 fs). Figure 2 shows the results of our simulations for 1PEF and 2PEF Lidars in the case of a 10 m diameter plume containing 100 bacteria/cm³, as a function of the distance between the plume and the Lidar system, for two ozone concentrations typical of urban atmospheres. This concentration determines the distance at which 2PEF becomes more efficient than 1PEF. In particular, 1PEF Lidar will not be practicable (limited to a few hundred meters) in urban conditions in summer, where average O₃ concentrations very often exceed 100 $\mu\text{g}/\text{m}^3$.

The simulations also provide estimations of the typical 2PEF-Lidar detection limits. As an example, for the average ozone concentration of 50 $\mu\text{g}/\text{m}^3$, we obtain a minimum detectable concentration (corresponding to 1 fluorescence photon/pulse) as low as 4 bacteria/cm³ at 3 km or 10 bacteria/cm³ at 4 km with a 10 m distance resolution. At these distances and ozone concentrations, 1PEF Lidar detection is almost useless. The estimated detection limit might strongly vary from one type of bacteria to another, because of the variations of the fluorescence quantum yield η [12]. Even for the values taken here [9], which corresponds to fluorescence measurements of *Bacillus Subtilis* and *Bacillus Cereus*, variations of up to an order of magnitude have been observed. These variations in η , however, affect the absolute detection limits for a type of bacteria, but not the 1PEF-2PEF Lidar comparison.

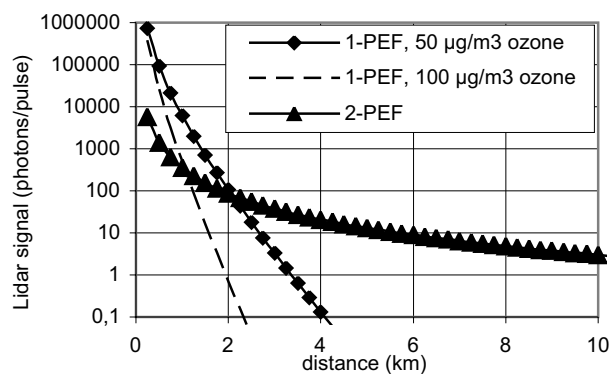


Figure 2: Simulated fluorescence Lidar signal for tryptophan detection in bioaerosols. The collected 2PEF intensity is higher than 1PEF for distances over 1-2 km, due to the lower atmospheric transmission in UV (Rayleigh scattering and ozone absorption, here typical cases of 50 and 100 $\mu\text{g}/\text{m}^3$)

2. FILAMENTS CAN PROPAGATE THROUGH CLOUDS

The main limitation of 2PEF Lidar is, however, the ability to deliver the required intensity at the target plume location. Recently, we showed that filamentation can reach distances of several kilometers [13]. However, a key problem is to deliver the filaments at the heart of the cloud, requiring that the filaments can be transmitted through cloud layers. To address this question, we observed the interaction of a light filament with a single, isolated water droplet. An ultrashort laser (7 mJ/pulse, 120 fs pulse duration at 810 nm) was slightly focused to produce a light filament of typically 150 μm in diameter, that can propagate over more than 3 m. The location of the onset of filamentation for each given laser power was defined as origin or the propagation distance d .

At $d = 1$ m, the light filament interacted with a calibrated micrometric water droplet of controlled diameter a , generated by a piezo-driven nozzle synchronized with the laser so that each laser pulse interacted with a single fresh droplet. We defined the impact parameter b , i.e. the distance between the filament axis and the center of the droplet. The experimental reproducibility on a and b , checked by both forward elastic scattering and direct observation with a microscope, was excellent: $\Delta b/a < 0.1$, $\Delta a/a < 0.05$.

We first measured the intensity profile of the freely propagating laser beam (i.e. without droplet), as shown in the insets to Fig. 3. Only a fraction of the energy was used to form the filament while the remaining laser energy surrounds this highly localized structure and propagates collimated with it. At the location where the interaction with the droplet occurs ($d = 1$ m) the filament

carries some 35 % of the total energy (2.7 mJ). 1 m further this fraction drops to $\sim 13\%$, and only 3 % (0.25 mJ) at $d = 3$ m. The surrounding "photon bath" (about 2 mm in diameter) accordingly gains energy with propagation and acts as an energy reservoir [14] that is in dynamic balance with the filament.

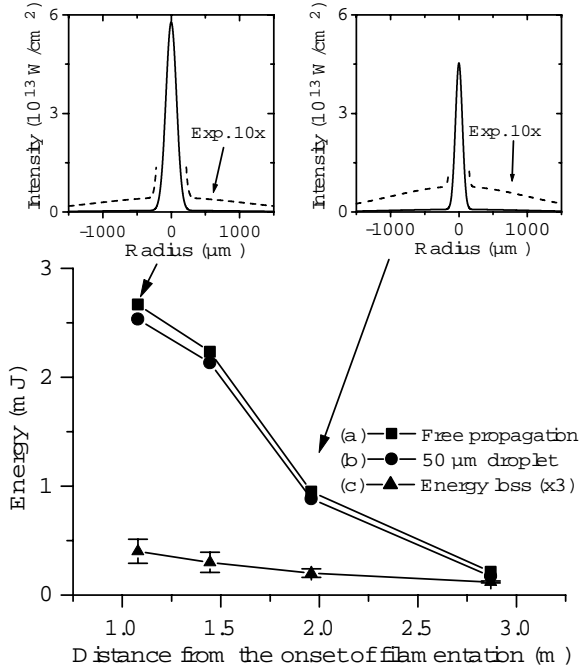


Figure 3. Interaction of a light filament with a $50\ \mu\text{m}$ water droplet. Energy contained in the filament as a function of propagation distance d (relative to the onset of filamentation at $d=0$): (a) without and (b) with droplet. The insets are measured intensity profiles of the freely propagating filament as a function of distance. Expanded scale curves (intensity $\times 10$, dashed line) show the contribution of the surrounding "photon bath". The filamentary structure globally loses energy to the surrounding photon bath. However, curve (c) displays the difference (a)-(b) (energy loss) and suggests that some energy is re-gained by the filament from the photon bath while propagating after the interaction with the droplet. The error bars in curve (c) account for statistical errors of the energy measurement only. Systematic errors of measurements with and without droplets are balanced since the same foil is used.

A $50\ \mu\text{m}$ diameter water droplet was precisely placed in the center of the filament at $d=1$ m. Surprisingly, the filament was completely unaffected by the presence of the droplet even though the balance between Kerr self-focusing and defocusing by the self-generated plasma should be highly critical because of the non-linear nature of the processes. In order to better understand this remarkable result, the energy carried by the filament along the direction of propagation (Fig. 3,

curve b) was measured in the same way as for the free propagation. A slight energy loss of 130 ± 40 mJ is observed just after the interaction ($d = 1$ m) but the balance is quickly re-established. The filament seems to re-gain energy, i.e. to be replenished by the surrounding photon bath while it continues to propagate (Fig. 3, curve c). Theoretical predictions [14,15] depicting non-linear propagation processes of ultra-short laser pulses corroborate this interpretation of a dynamic energy balance between the filament and the surrounding energy bath. Similar results were obtained with bigger droplets (up to $95\ \mu\text{m}$), as well as with opaque particles.

Since the filament has to be replenished by the photon bath, the transmission of the latter through the cloud is critical. To address this question, we launched the filament through an open cloud chamber of 0.35 m length and measured the transmitted energy. We monitored the droplet size distribution using forward Mie scattering (mean diameter $4\ \mu\text{m}$, FWHM = $2\ \mu\text{m}$), and the cloud optical thickness (COT) τ with the transmission of a He:Ne laser.

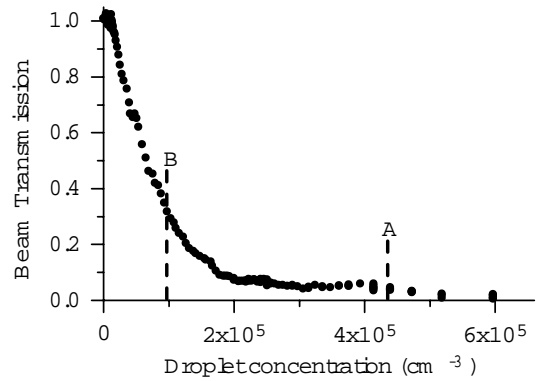


Figure 4. Transmission of light filaments through a cloud (droplet mean diameter $4\ \mu\text{m}$, FWHM = $2\ \mu\text{m}$). The filaments propagate throughout the cloud for an optical thickness τ as high as 3.2 (droplet concentration $4 \cdot 10^5\ \text{cm}^{-3}$, label A). However, it does not further propagate on emerging from the cloud because the energy loss in the photon bath by elastic scattering is too high. Conversely, almost unaltered filamentation is observed for $\tau = 1.2$ ($10^5\ \text{cm}^{-3}$, label B).

As shown in Fig. 4, the filament propagates throughout the cloud, even for an optical thickness τ as high as 3.2 (corresponding to a droplet concentration of $4 \cdot 10^5\ \text{cm}^{-3}$). However, after a few cm of further propagation in clear air, filamentation stopped. The reason for this behaviour is the energy loss in the photon bath due to elastic scattering. At the cloud exit the energy is no longer sufficient to enable further propagation of the filament. The transmitted power in the beam is only 2.3 GW,

which is lower than the power P_c needed for Kerr focusing.

Conversely for an optical thickness of 1.2 (10^5 droplets/cm³) the filament is fully transmitted and further propagates almost unaffected, since the filamentation length is close to the one in clear air.

Notice that the filament transmission exponentially decreases with the droplet concentration (Fig. 4), as expected for linear scattering. This indicates that the energy loss in the photon bath by Mie scattering dominates the process and constitutes the main limitation for filament transmission through clouds. However, the maximum optical thickness measured in our experiments corresponds to values typical of cumulus or stratocumulus clouds. These results are most promising, particularly when taking into consideration the modest laser energy (7 mJ). Using a higher energy, the penetration depth into the cloud will be even longer, allowing for remote diagnostics of the cloud core for biological aerosols. Moreover, shaping the pulses in 2PEF experiments and using genetic algorithms moreover recently showed that two species exhibiting the identical linear fluorescence spectrum [7] can be efficiently distinguished. This remarkable experiment opens new perspectives in identifying bioagents from other fluorescing particles using 2PEF-Lidars, even at the heart of clouds.

ACKNOWLEDGEMENTS

Teramobile is a French-German project jointly funded by the CNRS and the DFG. The authors wish to thank Steven C. Hill at ARL, Adelphi (MD), Prof. S.L. Chin (Laval University), Prof. M. Beniston (Univ. Freiburg, Switzerland) and Dr. A. Ross (Univ. Lyon 1) for very fruitful discussions, Marc Néri and M. Kerleroux for helpful technical support, and Matthieu Jomier for assistance in preparing Figure 3

REFERENCES

- 1 J. Kasparian, M. Rodriguez, G. Méjean, J. Yu, E. Salmon, H. Wille, R. Bourayou, S. Frey, Y.B. Andre, A. Mysyrowicz, R. Sauerbrey, J.P. Wolf, L. Woeste, *Science* **301**, 61-64 (2003)
- 2 H. Wille, M. Rodriguez, J. Kasparian, D. Mondelain, J. Yu, A. Mysyrowicz, R. Sauerbrey, J.P. Wolf, L. Woeste, *European Physical J. D* **20**(3) 183-189 (2002)

- 3 S. C. Hill, V. Boutou, J. Yu, S. Ramstein, J.P. Wolf, Y. Pan, S. Holler, R. K. Chang, *Phys.Rev.Lett.* **85**(1), 54-57 (2000)
- 4 Y.S. Cheng, E.B. Barr, B.J. Fan, P.J. Hargis, D.J. Rader, T.J. O'Hern, J.R. Torczynski, G.C. Tisone, B.L. Preppernau, S.A. Young, R.J. Radloff, S.L. Miller, J.M. Macher, *Aerosol Science and Technology* **30**, 186-201 (1999)
- 5 J.P. Wolf, Y. Pan, S. Holler, G. M. Turner, M. C. Beard, R.K. Chang, A.Schmittenmaer, *Phys.Rev. A* **64**, 023808-1-5 (2001)
- 6 L. Méès, J.P. Wolf, G. Gouesbet, G. Gréhan, *Optics Comm.* **208** 371-375 (2002)
- 7 T. Brixner, N. Damrauer, P. Niklaus, G. Gerber, *Nature* **414**, 57-60 (2001)
- 8 R.J. Levis, G.M. Menkir, H. Rabitz, *Science* **292**, 709-713 (2001)
- 9 G.W. Faris, R A Copland, K. Mortelmans, B. V. Bronk, *Applied Optics* **36**(4), 958-967 (1997)
- 10 S.C. Hill, R. G. Pinnick, S. Niles, Y. L. Pan, S. Holler, R. K. Chang, J. R. Bottiger, B. T. Chen, C. S. Orr, G. Feather, *Field Anal. Chem. Technol.* **3** (4-5), 221 (1999)
- 11 M. Lippitz, W. Erker, H. Decker, K.E. van Holde, T. Basche, *Proc. National Academy of Sciences* **99**(5), 2772-2777 (2002)
- 12 A. Rehms, P. Callis, *Chemical Physics Letters* **208**, 276-282 (1993)
- 13 M. Rodriguez, R. Bourayou, G. Méjean, J. Kasparian, J. Yu, E. Salmon, A. Scholz, B. Stecklum, J. Eislöffel, U. Laux, A. P. Hatzes, R. Sauerbrey, L. Wöste and J.-P. Wolf, to be published in *Physical Review E* (2004)
- 14 M. Mlejnek, E. M. Wright, J. V. Moloney, *Optics Letters* **23**, 382 (1998)
- 15 M. Mlejnek, E. M. Wright, J. V. Moloney, *Optics Express* **4**, 223 (1999)